Biochimica et Biophysica Acta 899 (1987) 83–92
Elsevier

BBA 73538

Fast reversal of the initial reaction steps of the plasma membrane (Ca^{2+} + Mg^{2+})-ATPase

José D. Cavieres

Department of Physiology, Leicester University, University Road, Leicester, LE1 7RH (U.K.)

(Received 2 December 1986)

Key words: Calcium pump; ATP–ADP exchange; Magnesium ion; Calmodulin; Erythrocyte

(1) Calmodulin-depleted red cell membranes catalyse a Ca^{2+}, Mg^{2+}-dependent ATP–[^{3}H]ADP exchange at 37°C. The Ca^{2+}, Mg^{2+}-dependent exchange, measured at 20 μM $CaCl_2$, 1.5 mM $MgCl_2$, 1.5 mM ADP and 1.5 mM ATP, is comparable to the (Ca^{2+} + Mg^{2+})-ATPase activity, between 0.3 and 0.8 mmol/litre original cells per h. (2) EDTA-washed membranes present a Ca^{2+}-dependent ATP–ADP exchange whose rate is not more than 7% of that found in a Mg^{2+}-containing medium, while their Ca^{2+}-dependent ATPase is essentially zero. Addition of 1.5 mM $MgCl_2$ to the medium restores both activities to the levels found with membranes not treated with EDTA. (3) Calmodulin (16 μg/ml) produces an eight-fold stimulation of the Ca^{2+}-dependent ATP–ADP exchange, slightly less than it stimulates the Ca^{2+}-dependent ATP hydrolysis. The effect of 1.5 mM $MgCl_2$ on the exchange is greater in the presence than in the absence of calmodulin. (4) It is proposed that the reversal of the initial phosphorylation of the Ca^{2+} pump, occurring at a fast rate at 37°C, involves a conformational change in the phosphoenzyme. Thus, it would be an ADP-liganded phosphoenzyme of the form EP(ADP) that would experience the fast conformational transition at 37°C. The great difficulty in producing an overall reversal of the Ca^{2+} pump should then be due to one or more reaction steps later than and including Ca^{2+} release and dephosphorylation.

Introduction

Red cells pump Ca^{2+} outwards against a very steep electrochemical gradient [1], coupling the translocation to a Ca^{2+}-dependent ATPase activity of their membranes [2]. The Ca^{2+} pump has now been described in a number of other tissues and cells [3,4] and its activity can be greatly stimulated by calmodulin (CaM) [5]. Purified preparations of (Ca^{2+} + Mg^{2+})-ATPase can transport Ca^{2+} in the presence of ATP when reconstituted in artificial phospholipid vesicles [6].

It is currently accepted that the reaction cycle of the plasma membrane Ca^{2+} pump occurs via the formation and breakdown of phosphorylated intermediates. The red cell pump is phosphorylated by ATP in the presence of calcium ions, both acting at high-affinity sites [7,8]. The phosphoenzyme thus formed (E_1P) breaks down only slowly at 0°C, and a conformational change seems necessary to produce another form (E_2P) which is hydrolysed at a rate compatible with the overall ATPase reaction [9]. Magnesium ions seem indispensable for this conversion and that may explain

Abbreviations: EGTA, ethylene glycol bis(β-aminoethyl ether)-*N*,*N*,*N*′,*N*′-tetraacetic acid; Hepes, 4-(2-hydroxyethyl)-1-piperazineethanesulphonic acid.

Correspondence: J.D. Cavieres, Department of Physiology, Leicester University, University Road, Leicester, LE1 7RH, U.K.

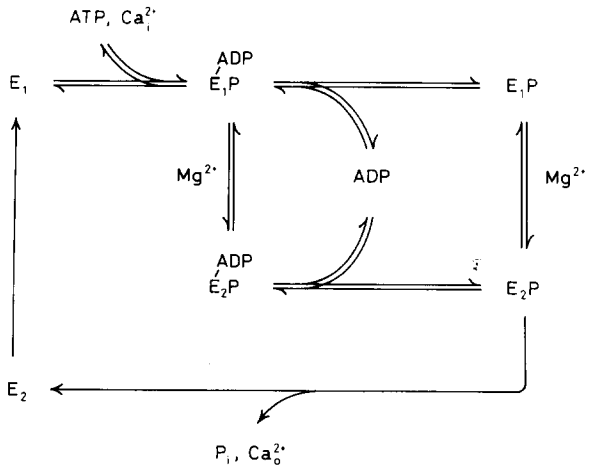

Fig. 1. The red cell pump.

their requirement for ATP hydrolysis and Ca^{2+} transport. This is represented by the external circuit of Fig. 1.

In the presence of ADP and Ca^{2+}, an increase in the dephosphorylation rate can be observed at 0 °C [10,11], and this has been interpreted as a reversal of the initial phosphorylation. Since it seemed worthwhile studying this initial partial reaction at 37 °C, it was decided to find out whether a Ca^{2+}-dependent ATP–ADP exchange could be measured. ATP–ADP exchange represents the steady-state expression of a reversible phosphorylation and can be followed as the incorporation of ^3H label of [^3H]ADP into ATP. The isotopic exchange should come to equilibrium when the specific activities of [^3H]ATP and [^3H]ADP become equal, i.e. when the fractional ^3H in ATP equals the ATP concentration expressed as [ATP]/([ATP] + [ADP]). This 'relative ATP concentration', which represents the equilibrium or infinity value for the exchange is, however, an ever decreasing value because of concomitant ATP hydrolysis. To allow for this, [γ-^{32}P]ATP can also be introduced in the reaction medium, to measure the rate of [^{32}P]P_i release simultaneously and in the same tubes [12].

According to the scheme which emerged from the phosphorylation experiments (outer circuit in Fig. 1), the partial reactions catalysing ATP–ADP exchange should be inhibited or unaffected by magnesium. The experiments in this paper were designed to test this prediction. A Ca^{2+}-sensitive ATP–ADP exchange could indeed be measured, but the Mg^{2+} effect was exactly the opposite as expected. Calmodulin, besides, was found to produce a large stimulation of the Ca^{2+}-sensitive ATP–ADP exchange. A possible explanation for these results is that the conformational change in the phosphoenzyme at 37 °C occurs mostly on a species which has ADP still bound to it. This is illustrated by the internal circuit in Fig. 1. Preliminary reports have been published [13,14].

Methods

Experimental protocols

Calmodulin-depleted membranes form human red cells were prepared from bank blood as already described [15,16] and stored in aliquots at −20 °C at an equivalent 200% haematocrit and in a solution containing (mM): Hepes 5 (adjusted to pH 7.4 with NaOH), $MgCl_2$ 0.1. The ghosts were thawed just before use. If a Mg^{2+}-free condition was required, they were diluted with at least 10 volumes of a chilled solution containing (mM): Hepes 5, EDTA 5 (adjusted to pH 7.4 with NaOH) and spun out for 30 min at 27000 × g in a 15-ml polycarbonate tube (r_{av} = 7.6 cm) at 5–8 °C. The pellet was resuspended and washed twice with cold 5 mM Hepes (Na) (pH 7.4) and finally made up to an equivalent 100% haematocrit with 5 mM Hepes. The membranes then received $CaCl_2$ and ouabain (to inhibit the Na^+ pump), so that their final concentrations during the 37 °C incubation were 20 μM and 0.1 mM, respectively. At this stage, the membrane suspension was divided into several lots which did or did not receive concentrated solutions of $MgCl_2$ or calmodulin, so that their final concentrations were 1.5 mM and 16 μg/ml, respectively. When calmodulin was included, all suspensions were pre-incubated for 5 min at 37 °C, to allow plenty of time for calmodulin binding.

Time-course experiments were carried out by mixing at timed intervals, at 37 °C, the various membrane lots with (a) a solution containing ADP (plus [^3H]ADP), ATP (plus [γ-^{32}P]ATP), NaCl and KCl, made up in 5 mM Hepes (Na) (pH 7.4), so that the final concentrations were (mM): 1.5, 1.5, 50 and 50, respectively, or (b) a similar solution, but also containing EGTA to give a final

concentration of 0.5 mM. 40 μl of the suspensions were sampled into microcentrifuge tubes at various times and the tubes were kept for 2 min in a boiling-water bath and cooled down on iced water. In the case of 'initials-and-finals' experiments, individual microcentrifuge tubes were filled on an ice bath with aliquots of the membrane lots and of the solution containing the nucleotides. The total volume was 40 μl. The 'finals' were transferred to the 37 °C bath as the 'initials' were boiled, the 'finals' being boiled after a 30 min incubation. In all experiments, the membrane contents in the final incubation represented 30% haematocrit on the original cells' volume.

Processing of the samples

The separation of nucleotides and P_i was done by thin-layer chromatography on fluorescent polyethyleneimine-cellulose sheets [17], after addition of carriers (including AMP). To obtain consistent clear-cut separations: (a) the sheets (mounted on glass plates with double-sided tape) were scored to form tracks 15 mm-wide and the samples (15 μl) were applied with a piece of glass cover-slip, so as to obtain a broad thin band and (b) the rack with the plates were equilibrated for 45 min in the sealed tank, suspended over the mobile phase (1.2 M LiCl), before immersing. To speed up the elution procedure, the eluant (0.7 M $MgCl_2$) was supplemented with 12.5 mM sodium acetate, the pH being adjusted to 5.5 with HCl. The cuttings were placed inside plastic scintillation-vial inserts with 1.2 ml of this solution, and racks with the inserts were shaken mechanically for 30 s, inverted and shaken again; this routine yielded a quantitative recovery of radioactive label from test spots. The inserts were then centrifuged for 2 min at $3000 \times g$ and 0.5-ml samples were withdrawn and mixed with 4.5 ml of a solution consisting of 8 parts of Biofluor (New England Nuclear) and one part of absolute ethanol. This system goes into one phase below 10 °C in the scintillation counter.

Each of the eluted fractions (ATP, ADP, and AMP/P_i) was counted for ^3H and ^{32}P in a Packard Tri-Carb Scintillation Spectrometer. The channels were set so that no ^3H counts collected in the ^{32}P channel; the ^{32}P overspill into the ^3H channel (about 1%) was measured each time with a ^{32}P standard, and the sample activities were chosen so that this correction did not represent more than about 20% of the counts in the ^3H channel in the earliest ATP fractions. Whenever possible, 10000 counts were collected. For the calculations, the [^3H]ATP activity was expressed as a fraction of the total ^3H counts recovered for the sample (i.e., the sum of ^3H counts in the ATP, ADP and AMP/P_i fractions); likewise, the [^{32}P]P_i activity was expressed as a fraction of the total ^{32}P in the sample.

In a few instances, the TLC plates were scanned for radioactivity along the entire length of each of the sample tracks. A Panax Thin Layer Scanner (RTLS-1A), fitted with a windowless gas flow detector, was used to that purpose.

Calculations

In the case of progress curves, the rate constant for the back reaction of ATP–ADP exchange (k'_{-1}) was obtained from plots of $\ln(1 - y/y_\infty)$ vs. time (Eqn. 3 of the Appendix), where y_∞ on the left-hand side is the relative ATP concentration (R = [ATP]/([ATP] + [ADP])). R was calculated with Eqn. 5, which allows for ATP hydrolysis with the aid of the ^{32}P data. Thus, k'_{-1} is given by $-R_{av}$ times the slope of the semilogarithmic plot, where R_{av} is the average relative ATP concentration during the experiment. For experiments with 'initial' and 'final' tubes, the rate constant was obtained with Eqn. 7. The ATP–ADP exchange activity was obtained by multiplying k'_{-1} by the ADP concentration and referred to the haematocrit (in terms of volume of original cells). Standard errors were estimated as described in the Appendix.

Materials

ATP (disodium salt) and ADP (free acid) were purchased from Boehringer Mannheim and all other biochemicals, including bovine brain calmodulin, from Sigma. The thin-layer chromatography sheets (Polygram, CEL 300 PEI/UV_{254}) were from Machery-Nagel. [2-^3H]ADP (22 C_i/mmol) was bought from Amersham International and the [γ-^{32}P]ATP (10 C_i/mmol) was prepared by a modification of the method by Glynn and Chappell [18], from [^{32}P]orthophosphoric acid supplied by New England Nuclear. Working solu-

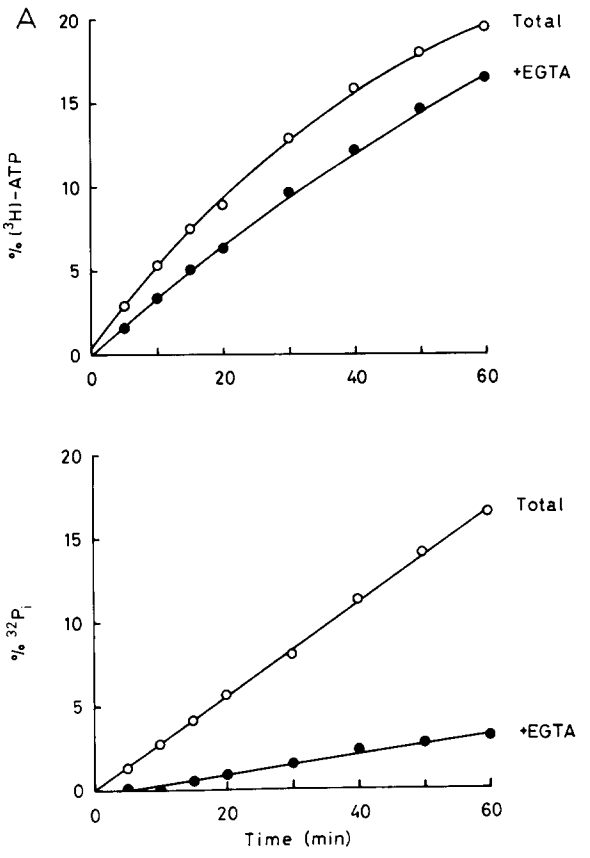

Fig. 2. Progress curves of ATP–[^{3}H]ADP exchange and [γ-^{32}P]ATP hydrolysis of calmodulin-depleted red cell membranes, running simultaneously in the presence of 20 μM $CaCl_2$, and 0.1 mM ouabain. 'Total' is meant for the standard condition (see Methods); EGTA was at 0.5 mM (final concentration). (A) With 1.5 mM $MgCl_2$. Upper panel: incorporation of ^{3}H label from [^{3}H]ADP into ATP, as per cent of the total ^{3}H (i.e. 100×fractional [^{3}H]ATP) in the 40 μl sample. The curves have been drawn using Eqn. 6 with the parameters from the fitting of Fig. 3 and the lower panel of Fig. 2A. Lower panel: release of [^{32}P]P_i from [γ-^{32}P]ATP, as per cent of the total ^{32}P in the sample. The straight lines' parameters were obtained by least-squares fitting. The linear regression coefficients (hydrolysis rate constants, H) as mean ±S.E., are (h^{-1}): 0.1640±0.0018 (Total), 0.0360±0.0019 (+EGTA). Each point on the lower panel arises from the same sample as the corresponding point on the upper panel. (B) Other two progress curves from the same experiment, but run in the absence of $MgCl_2$ and plotted separately for the sake of clarity. All other conditions are similar, but notice the expanded ordinate axes. From the linear regression coefficients in the lower panel, the hydrolysis rate constants, calculated as mean ±S.E., are (h^{-1}): 0.0056±0.0017 (Total), 0.0090±0.0028 (+EGTA). The rate constants for ATP–ADP exchange (obtained through plots similar to those of Fig. 3, as mean ±S.E. are (h^{-1}): 0.0063±0.0007 (Total), 0.0030±0.0009 (+EGTA).

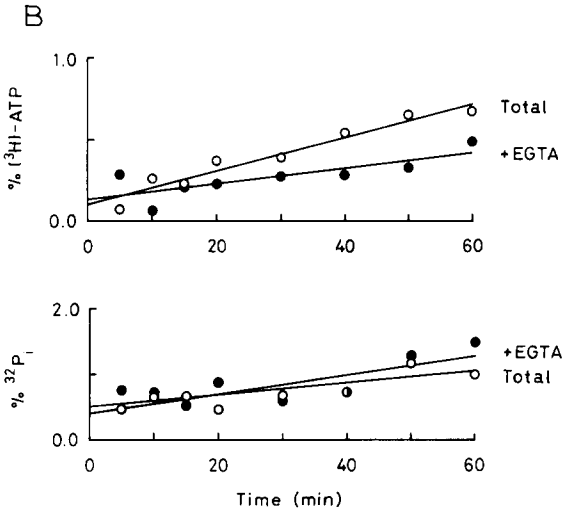

tions were prepared by taking up the radioisotopes with the non-radioactive nucleotide solutions, after the 50% ethanol used for storage had been blown off by a stream of nitrogen.

Results

Fig. 2 and the first two rows of Table I show the result of one of several time-course experiments to reveal a Ca^{2+}-dependent ATP–ADP exchange and the effect of Mg^{2+} on it. Fig. 2A shows the results obtained in the presence of 1.5 mM Mg^{2+} and Fig. 2B, those in its absence. The ATPase activities and their errors are calculated from the regression coefficients (and their errors) for the fitted straight lines in the lower panels in Fig. 2, from the ATP concentration (1.5 mM) and the final membrane concentration (30% heamatocrit on the original cells).

From Fig. 2A, it is evident that there is a sizeable Ca^{2+}-dependent component of ATP–ADP exchange in the presence of Mg^{2+}. It is also apparent that the two [^{3}H]ATP curves tend to converge on each other towards the end of the incubation period. This effect is due to the high ATPase rate associated with the condition marked 'total' with respect to that marked '+EGTA' (cf. lower panel), which makes the upper exchange curve deviate in a downward direction, 'aiming' at steady decreasing equilibrium values on account of the decreasing relative ATP concentration. To

visualize the true course of ATP–ADP exchange and obtain its rate constant, the data of the upper panel in Fig. 2A were replotted in semilogarithmic form for approach to equilibrium, whilst being corrected for hydrolysis (Eqn. 3 of the Appendix), and are shown in Fig. 3. Here y is the fractional [^{3}H]ATP level and y_∞ is estimated by R, the relative ATP concentration, initially 0.5 in the present experiments. The declining value of R has been calculated for each sampling time in each curve with the aid of the ATP hydrolysis rate constant, obtained with the fitting in the lower panel of Fig. 2A. In calculating R by this means (see legend to Fig. 3), it is assumed that the ATP hydrolysis is linear with time during the incubation period, which is justified according to the ^{32}P data of Fig. 2A, and that no ADP is hydrolysed. The latter assumption seems also correct, because there was no consistent increase in the fractional [^{3}H]AMP during the incubations and no fast-migrating species (adenosine, inosine) were detected in radioactivity scans of the TLC plates.

Good linear fittings were obtained for the secondary plots in Fig. 3. (The least-squares regressions on these semilogarithmic arrays give more weight to the smaller values of $(1 - y/y_\infty)$ but then they arise from the higher, and hence more reliable, y values). With the rate constants (k'_{-1}) obtained from the slopes, the ATP–ADP exchange activities were calculated as described under Methods and the Ca^{2+}-dependent components of both exchange and ATPase activities are shown on the first row of Table I.

The other half of Expt. 1, with the same EDTA-washed membrane suspension but without added $MgCl_2$, is shown, for clarity, in Fig. 2B. A similar semilogarithmic transformation of the [^{3}H]ATP data (not shown) led to the ATP–ADP exchange activities under '$-MgCl_2$' in Table I; the ATPase rates were calculated as for Fig. 2A. Evidently, the Ca^{2+}-dependent ATPase activity is essentially zero whereas, despite the large error attending such low rates, there is still a very small yet significant Ca^{2+} – dependent ATP–ADP exchange ($P < 0.02$). This can also be appreciated from Fig. 2B. But the more important and clearer conclusion is that 1.5 mM $MgCl_2$ produces a very large stimulation of the Ca^{2+}-dependent ATP–ADP exchange.

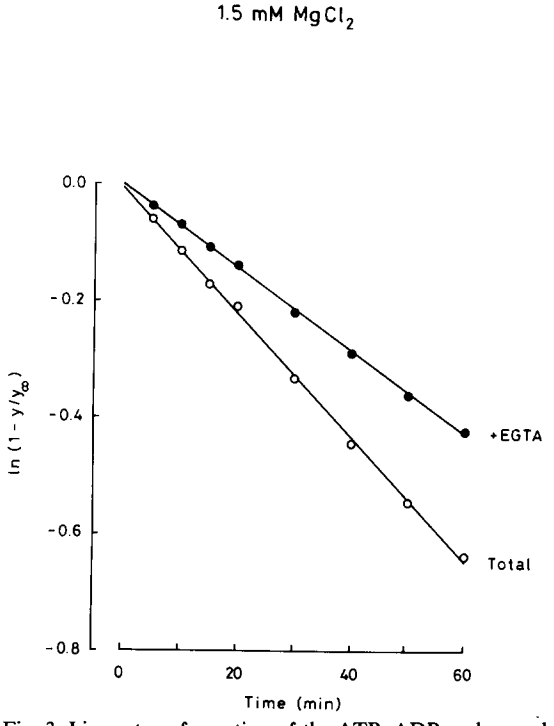

Fig. 3. Linear transformation of the ATP–ADP exchange data of Fig. 2A (upper panel). The fractional [^{3}H]ATP (percent value from Fig. 2A divided by 100) is y, and y_∞ is each of the equilibrium values. 'Instant' y_∞ values were obtained as the product of the initial relative ATP concentration (0.5 in these experiments) and the breakdown factor $(1 - H \cdot t)$, where H is the hydrolysis rate constant (in min^{-1}) and t is time in min. Straight lines of the form $\ln(1 - y/y_\infty) = a \cdot t + b$ were fitted by least squares. Rate constants were calculated from the regression coefficients (a) and the average R value (R_{av}). The rate constants as mean ±S.E., are (h^{-1}): 0.2956±0.0047 (Total) and 0.2104±0.0027 (+EGTA).

The ATP–ADP exchange curves in Fig. 2 were drawn with Eqn. 6 of the Appendix, where a and b were the fitted parameters for straight lines as in Fig. 3, and H was the hydrolysis rate constant for the respective condition obtained from the lower panels of Fig. 2. Similar calculations showed that if the ATPase activity of the 'total' curve in Fig. 2 had been as low as that of the '+EGTA' curve in the same figure, the % [^{3}H]ATP at 30 and 60 min would have been higher by 7.2% and 15.7% of the observed values, respectively. Because of the large Ca^{2+}-independent component, this effect is magnified when considering the Ca^{2+}-dependent % [^{3}H]ATP difference; at 30 and 60 min, this would

TABLE I

THE MAGNITUDES OF THE Ca^{2+}-DEPENDENT ATP–ADP EXCHANGE AND ATPase ACTIVITIES AND THE EFFECT OF $MgCl_2$

Enzymic activities in mmol/l original cells per h (mean ± S.E.). Summary of three time-course experiments to measure ATP–[^{3}H]ADP exchange and [γ-^{32}P]ATP hydrolysis at 20 μM $CaCl_2$, with and without 0.5 mM EGTA Expt. 1 is that of Figs. 2 and 3. In Expts. 2 and 3 there was no pre-wash with EDTA and the reactions were followed up to 30 min at 37 °C (seven time points). Where present, $MgCl_2$ was at 1.5 mM.

	$MgCl_2$	Ca^{2+}-dependent ATP–ADP exchange	Ca^{2+}-dependent ATPase activity
Expt. 1	+	0.426 ± 0.027	0.655 ± 0.013
	−	0.017 ± 0.006	−0.017 ± 0.016
Expt. 2	+	0.495 ± 0.088	0.855 ± 0.033
Expt. 3	+	0.608 ± 0.138	0.848 ± 0.033

TABLE III

THE EFFECT OF $MgCl_2$ WHEN THE EDTA WASH IS FOLLOWED BY TWO $CaCl_2$ WASHES

Enzymic activities in mmol/l original cells per h (mean ± S.E.). After an initial EDTA wash (see Methods), the membranes were resuspended with 25 vols. of cold 1 mM $CaCl_2$, 5 mM Hepes (Na) (pH 7.4) and centrifuged for 30 min at 27000 × g. After one more wash with this solution, the membranes were washed twice with cold 5 mM Hepes (Na) (pH 7.4) packed and resuspended with 5 mM Hepes. ATP–ADP exchange and ATPase activities were then measured in triplicate 'initials' and 'finals' (0 and 30 min), in the standard conditions. Where indicated, $MgCl_2$ was added to a final concentration of 1.5 mM.

$MgCl_2$	Ca^{2+}-dependent ATP–ADP exchange	Ca^{2+}-dependent ATPase activity
+	0.807 ± 0.029	0.943 ± 0.025
−	0.045 ± 0.011	0.014 ± 0.026

have been higher by 28% and 201% of the observed differences, respectively.

It was possible that a Mg^{2+} requirement for Ca^{2+}-dependent ATP–ADP exchange was peculiar to the calmodulin-depleted (Ca^{2+} + Mg^{2+})-ATPase. Therefore, an experiment was done to find out whether Mg^{2+} was still required when the enzyme was being stimulated by calmodulin. Its result is presented in Table II. It is quite evident that 1.5 mM Mg^{2+} produced a large Mg^{2+} stimulation of the Ca^{2+}-sensitive exchange in the presence of calmodulin (bottom two rows), even greater than in its absence. However, calmodulin stimulated the Ca^{2+}-dependent ATP–ADP exchange less than it did the Ca^{2+}-dependent ATPase activity (compare second and fourth rows). Besides, there was a small but significant Ca^{2+}-dependent ATP–ADP exchange but no Ca^{2+}-dependent ATPase activity in the absence of Mg^{2+} and calmodulin, confirming the results of Fig. 2; the addition of 1.5 mM MgCl increased both activities to roughly the same level (first two rows).

TABLE II

THE EFFECTS OF $MgCl_2$ AND CALMODULIN ON THE Ca^{2+}-DEPENDENT ATP–ADP EXCHANGE AND ATPase ACTIVITIES

Enzymic activities in mmol/l original cells per h (mean ± S.E.). Both ATP–ADP exchange and ATPase activities were measured in EDTA-washed membranes in triplicate 'initial' and 'final' tubes (0 and 30 min), at 20 μM $CaCl_2$ and with and without 0.5 mM EGTA. Where indicated, calmodulin was added at 16 μg/ml and $MgCl_2$ at 1.5 mM (final concentrations). CaM, calmodulin.

Mg^{2+}	CaM	Ca^{2+}-dependent ATP–ADP exchange	Ca^{2+}-dependent ATPase activity
−	−	0.020 ± 0.002	−0.001 ± 0.017
+	−	0.309 ± 0.033	0.355 ± 0.044
−	+	0.076 ± 0.003	0.105 ± 0.013
+	+	2.500 ± 0.140	4.944 ± 0.076

Finally, a possibility that the Mg^{2+} requirement for the exchange might have been artefactual was considered. An artefact could have arisen if some of the EDTA used in the wash had been left contaminating the membranes despite the subsequent Hepes wash, not just in the pellet's trapped volume (which was negligible) but, perhaps, binding to the membranes. This contaminating EDTA could have chelated all of the 20 μM Ca^{2+} added for the final incubation, except for a very small proportion bound to ATP and ADP. Thus, with EDTA-washed membranes not receiving supplementary $MgCl_2$, nearly identical ATP–ADP exchange activities would have been observed with and without 0.5 mM EGTA, i.e. a very small Ca^{2+}-dependent component would have been inferred. With 1.5 mM $MgCl_2$ during the final incubation, however, the bound Ca would have

been released from EDTA by the Mg^{2+} mass-action. The released Ca^{2+} – either as such or because of its nucleotide complexes – would have supported a large Ca^{2+}-dependent ATP–ADP exchange, which might not have had a Mg^{2+} requirement, thus creating the artefact. To eliminate this possibility, the experiment presented in Table III was performed. In this case, two washes with 1 mM $CaCl_2$ were interposed between the EDTA wash and the final Hepes wash. This procedure should saturate or release any 'bound' EDTA which might otherwise have been saturated or released by Ca^{2+} or Mg^{2+} during the final incubation. The results show a Mg^{2+} stimulation of the Ca^{2+}-dependent ATP–ADP exchange (and ATPase activity), which is comparable to that found with the other experiments. The Mg^{2+} requirement seems, therefore, genuine.

Discussion

The experiments presented above demonstrate the existence of a Ca^{2+}-dependent ATP–ADP exchange in red cell membranes at 37 °C, activity which most likely represents a reversal of the initial phosphorylation of the Ca^{2+} pump. They show, besides, that this ATP–ADP exchange has a requirement, though not absolute, for Mg^{2+} and that it can be stimulated by calmodulin.

The method used includes a measurement of the ATPase activity concomitant with the exchange for each of the experimental conditions, which is carried out simultaneously and in the same tubes. The importance of the appropriate correction for hydrolysis is borne out by comparing Figs. 2A and 3; the situation would have been worse for a case of just initial and final observations. It is not possible to predict when can a correction be dispensed with, since no safe correlation between ATP–ADP exchange and ATPase activity can be assumed when one is subjecting the system to various manipulations. The only acceptable alternative may be to keep the level of hydrolysis well below, say, 5% and ensure that it is the same for all the conditions to be compared.

The Mg^{2+} effect on ATP–ADP exchange is at odds with the published observations of its effects on phosphorylation and dephosphorylation at 0 °C (depicted by the external path of Fig. 1). Rega and Garrahan [10] and Schatzmann and Bürgin [11] have described an increase in the dephosphorylation rate caused by ADP in the presence of Ca^{2+}, presumably due to reversal and ATP resynthesis. The first authors found that such ADP-induced dephosphorylation occurred at the same rate whether or not 0.5 mM Mg^{2+} was present during phosphorylation, and this should have resulted in a lack of effect of Mg^{2+} on the Ca^{2+}-dependent ATP–ADP exchange. The Mg^{2+} requirement for ATP hydrolysis at 0 °C seems to arise during the interconversion of both phosphoenzymes, and not later, because the dephosphorylation rate is not affected if Mg^{2+} is removed from the medium simultaneously with the onset of dephosphorylation [9].

The present results could be reconciled with the phosphorylated intermediate cycle if it is assumed that, at 37 °C, the conformational change in the phosphoenzyme occurs while ADP is still bound to it. This is represented by the internal circuit in Fig. 1, where Mg^{2+} appears having the same effect on the conformational change of $E_1P(ADP)$ as in the transition of E_1P. The small Ca^{2+}-sensitive ATP–ADP exchange observed in the absence of Mg^{2+} (Fig. 2B and Tables I–III) could then be ascribed to some flux still taking place at 37 °C through the external path.

Rega and Garrahan [10] found a rate constant for (ADP + Ca^{2+})-induced dephosphorylation at 0 °C of between 0.4 and 0.5 s^{-1}. From Tables I–III of the present results, an average Ca^{2+}-dependent, Mg^{2+}-independent ATP–ADP exchange activity of 0.027 mmol/l original cells per h can be calculated. If one assumes a pump density of about 1000 sites per red cell [9,3] and a much larger proportion of E_1P than E_1 in the Mg^{2+}-free steady state, the backward-dephosphorylation rate constant (k_{-1}) in the absence of Mg^{2+} works out as 0.5 s^{-1}. As this is in close agreement with the figures obtained at 0 °C, it is tempting to hypothesize that whereas the rate of ADP re-binding to E_1P changes little or not at all with temperature, what increases very much at 37 °C is the reversible flow along $E_1P(ADP) \rightleftharpoons E_2P(ADP) \rightleftharpoons E_2P$ + ADP. This flow should increase from a value difficult to detect at 0 °C, say 10% of the rate through the external circuit, to between 15 and 30 times that rate (Tables I–III). This 300-fold in-

crease would imply a Q_{10} in the region of 4 to 5 for the rate-limiting step along the internal circuit, i.e. an activation energy of up to 108 kJ/mol. In studies on the temperature dependence of Ca^{2+} transport, an upper value of 104.6 kJ/mol has been reported [19].

The proposed new path for the reversible phosphorylation at 37 °C implies an alternative route for the overall ATPase and transport cycles. If the internal circuit were preferred for the overall ATPase reaction at 37 °C, the release of ADP, Ca^{2+} (to the external medium) and P_i would all occur from an E_2 conformer of the enzyme.

The $CaCl_2$ concentration was kept at 20 μM in the present study, in order to avoid possible self-inhibitory effects at higher concentrations (Wüthrich, quoted by, and Fig. 5 of, Ref. 3). The reversal of phosphorylation promoted by ADP at 0 °C does not seem to require a much higher Ca^{2+} concentration [10,11]. This raises the question as to why a Ca^{2+} requirement for reversal in those experiments, since much higher concentrations would have been required if low-affinity external Ca^{2+} sites had been involved [20]. Unless, of course, E_1P were also able to release Ca^{2+}, from sites of intermediate affinity. In the case of the ATP–ADP exchanges experiments, one would expect, at least, a high-affinity Ca^{2+} requirement because of the phosphorylation reaction. And since a high exchange rate was observed at just 20 μM $CaCl_2$, it is possible that calcium ions are released relatively slowly from E_2P, giving ADP ample opportunity to bind again before Ca^{2+} is lost at a low concentration to the 'external' medium. From the close correspondence of ATP–ADP exchange and ATPase rates in the presence of Mg^{2+}, it seems that the chances for E_2P to proceed forwards or backwards are nearly equally poised in these conditions.

The stimulation of the Ca^{2+}-dependent ATP–ADP exchange by calmodulin was not unexpected, since this peptide accelerates phosphorylation as well as dephosphorylation at 0 °C [15]. But there seems to be an additional effect, because Mg^{2+} produced a 15-fold stimulation of the Ca^{2+}-dependent ATP–ADP exchange in the absence of calmodulin, while it stimulated by a factor of nearly 33 in its presence (Table III). It is then possible that, besides Mg^{2+}, calmodulin also accelerates the conformational transition in the phosphoenzyme. What is clear is that up to that point all steps are readily reversible; the great difficulty in producing an overall reversal of the Ca^{2+} pump [21,22] should then be due to quasi irreversible steps involving $E_2P(Ca)$ and later enzyme forms.

Appendix

A generalised case for ATP–ADP exchange reactions can be stated as

$$\mathrm{ATP} + \mathrm{E} \underset{k_{-1}}{\overset{k_1}{\rightleftharpoons}} \mathrm{EP} + \mathrm{ADP} \tag{1}$$

where EP represents the sum of all enzyme forms reacting with ADP and E of those reacting with ATP.

If the appearance of [^{3}H]ATP as a fraction of total ^{3}H (henceforth called y) is measured against time and ^{3}H is distributed only between [^{3}H]ATP and [^{3}H]ADP

$$\frac{dy}{dt} = k'_{-1} \cdot (1 - y) - k'_1 \cdot y \tag{2}$$

where the operational rate constants are defined as $k'_{-1} = k_{-1}\mathrm{EP}$ and $k'_1 = k_1\mathrm{E}$. The solution is

$$\ln\left(1 - \frac{y}{y_\infty}\right) = -\frac{k'_{-1}}{y_\infty} \cdot t + b \tag{3}$$

where $-k'_{-1}/y_\infty$ is the slope a of the straight line and b is a constant. At $t = t_\infty$, the specific activities of [^{3}H]ATP and [^{3}H]ADP must be equal

$$\frac{y_\infty}{[\mathrm{ATP}]} = \frac{1 - y_\infty}{[\mathrm{ADP}]}$$

and

$$y_\infty = \frac{[\mathrm{ATP}]}{[\mathrm{ATP}] + [\mathrm{ADP}]} = R \tag{4}$$

and hence y_∞ represents the 'relative ATP concentration' (R). If the nucleotide concentrations are constant, Eqns. 3 and 4 will suffice. However, because of the ATPase activity y_∞ steadily decreases. If the ATP hydrolysis is linear with time during the observation period (up to, say,

20% hydrolysis)

$$R = R_0 \cdot (1 - H \cdot t) \tag{5}$$

where R_0 is the initial relative ATP concentration and H is the hydrolysis rate constant (min^{-1}). The latter can be obtained by regressing the release of [^{32}P]P_i from [γ-^{32}P]ATP linearly against time.

The y_∞ on the slope term of Eqn. 3 can be the average R for the observation period (R_{av}). The standard error on k'_{-1} can be estimated from the error on the regression coefficient of $\ln(1 - y/y_\infty)$ vs. t (the coefficient of variation (C.V.) on R_{av} is small compared to the C.V. on k'_{-1} and can be ignored). With progress-curve experiments, however, it is not readily apparent how the contribution of the error on R (for each time-point) should be considered for assessing the error in k'_{-1}.

The fitted parameters H, a and b can now be used to reconstruct the progress curve for ATP–ADP exchange. From Eqns. 3, 4 and 5

$$[^3\text{H}]\text{ATP} = 100\, R_0 (1 - H \cdot t)(1 - e^{a \cdot t + b}) \tag{6}$$

Alternatively, Eqn. 2 can be integrated between limits

$$\ln\left(\frac{1 - (y_1/y_\infty)}{1 - (y_2/y_\infty)}\right) = \frac{k'_{-1}}{y_\infty} \cdot (t_2 - t_1) \tag{7}$$

Eqn. 7 can be used to study the reaction with 'initial' and 'final' tubes. In this case, y_∞ in the numerator must be replaced by R_1 (at t_1) and in the denominator by R_2 (at t_2). The right-hand's y_∞ can be R_{av}. It is now possible to consider the variance introduced by the ATPase data in the estimate of the error of k'_{-1}, mainly through the R_1 and R_2 terms. If the propagation of the error is assessed with the reduction formula (6) of Wilkinson [23], the coefficient of variation on k'_{-1} is given by

$$\text{C.V.}(k'_{-1}) = \sqrt{\frac{A_1 + A_2}{B} + C} \tag{8}$$

where

$$A_i = \frac{Y_i}{(1 - Y_i)^2}\left(\frac{\text{SE}_i^2}{y_i^2} + \frac{t_i^2 \cdot h^2}{(1 - H \cdot t_i)^2}\right) \tag{8a}$$

$$B = \ln^2\left(\frac{1 - Y_1}{1 - Y_2}\right) \quad \text{and} \tag{8b}$$

$$C = \frac{h^2 \cdot (\Delta t)^2}{(2 - H \cdot \Delta t)^2} \tag{8c}$$

being $\Delta t = t_2 - t_1$, y = fractional [^{3}H]ATP, SE = S.E. on y, H = hydrolysis rate constant (min^{-1}), h = S.E. on H, $Y_i = y_i/R_i$ and $i = 1$ (initials) or 2 (finals). H is now calculated from the initial and final fractional [^{32}P]P_i.

Note added in Proof: (Received 30 March 1987)

On the basis of dephosphorylation experiments, Nakamura et al. ((1986) J. Biol. Chem. 261, 3090–3097) have recently proposed a branched pathway similar to that of Fig. 1, for the sarcoplasmic reticulum calcium pump.

Acknowledgements

I wish to thank Miss A. Gardner for her technical assistance and Mrs. J.A. Lewis and Mrs. C.M. Wright for their secretarial help.

References

1 Schatzmann, H.J. (1966) Experientia 22, 364–365
2 Dunham, E.T. and Glynn, I.M. (1961) J. Physiol. 156, 274–293
3 Schatzmann, H.J. (1982) in Membrane Transport of Calcium (Carafoli, E., ed.), pp. 41–108, Academic Press, New York and London
4 Michalak, M., Famulski, K. and Carafoli, E. (1984) J. Biol. Chem. 259, 15540–15547
5 Gopinath, R.M. and Vincenzi, F.F. (1977) Biochem. Biophys. Res. Commun. 77, 1203–1209
6 Niggli, V., Adunyah, E.S., Penniston, J.T. and Carafoli, E. (1981) J. Biol. Chem. 256, 395–401
7 Knauf, P.A., Proverbio, F. and Hoffman, J.F. (1974) J. Gen. Physiol. 63, 324–336
8 Katz, S. and Blostein, R. (1975) Biochim. Biophys. Acta 389, 314–324
9 Rega, A.F. and Garrahan, P.J. (1975) J. Membrane Biol. 22, 313–327
10 Rega, A.F. and Garrahan, P.J. (1978) Biochim. Biophys. Acta 507, 182–184
11 Schatzmann, H.J. Bürgin, H. (1978) Ann. NY Acad. Sci. 307, 125–146
12 Cavieres, J.D. (1983) in Current Topics in Membranes and Transport, Vol. 19, (Hoffman, J.F. and Forbush, III, B., eds.) pp. 677–681, Academic Press, New York and London
13 Cavieres, J.D. (1986) J. Physiol. 337, 85P

14 Cavieres, J.D. (1986) Biochem. Soc. Trans. 14, 1124–1125
15 Muallem, S. and Karlish, S.J.D. (1981) Biochim. Biophys. Acta 647, 73–86
16 Cavieres, J.D. (1984) Biochim. Biophys. Acta 771, 241–244
17 Randerath, K. and Randerath, E. (1967) in Methods in Enzymology, Vol. 12 A (Grossman, L. and Moldave, K., eds.), pp. 323–347, Academic Press, New York and London
18 Glynn, I.M. and Chappell, J.B. (1964) Biochem. J. 90, 147–149
19 Schatzmann, H.J. and Vincenzi, F.F. (1969) J. Physiol. 201, 369–395
20 Schatzmann, H.J. (1973) J. Physiol. 235, 551–569
21 Ferreira, H.G. and Lew, V.L. (1975) J. Physiol. 252, 86–87P
22 Wüthrich, A., Schatzmann, H.J. and Romero, P. (1979) Experientia 35, 1589–1590
23 Wilkinson, G.N. (1961) Biochem. J. 80, 324–332